View metadata, citation and similar papers at core.ac.uk
brought to you by CORE
provided by Publications of the IAS Fellows

arXiv:physics/0408015v1 [physics.chem-ph] 3 Aug 2004

Numerical simulation of transmission coefficient using c-number Langevin equation

Debashis Barik[1], Bidhan Chandra Bag[2] and Deb Shankar Ray[1*]
[1] *Indian Association for the Cultivation of Science, Jadavpur, Kolkata 700 032, India*
[2] *Department of Chemistry, Visva-Bharati, Santiniketan 731 235, India*
(Dated: February 2, 2008)

We numerically implement the reactive flux formalism on the basis of a recently proposed c-number Langevin equation [Barik *et al*, J. Chem. Phys. **119**, 680 (2003); Banerjee *et al*, Phys. Rev. E **65**, 021109 (2002)] to calculate transmission coefficient. The Kramers' turnover, the T^2 enhancement of the rate at low temperatures and other related features of temporal behaviour of the transmission coefficient over a range of temperature down to absolute zero, noise correlation and friction are examined for a double well potential and compared with other known results. This simple method is based on canonical quantization and Wigner quasiclassical phase space function and takes care of quantum effects due to the system order by order.

I. INTRODUCTION

The classic work of Kramers[1] on the diffusion model of classical reaction laid the foundation of the modern dynamical theory of activated processes. Since then the field of chemical dynamics has grown in various directions to extend the Kramers' result to non-Markovian friction[2,3], to generalize to higher dimensions[4,5] and to semiclassical and quantum rate theories[6,7,8,9,10,11,12,13,14,15,16,17,18,19] to apply extensively to biological processes[20] and to several related issues. An important endeavor in this direction is the formulation of reactive flux theory[9,19,21,26] which has been worked out in detail over the last two decades by several groups. The method is essentially based on the realization of rate constant of a chemical reaction as a Green-Kubo correlation function calculated at the transition state which acts as a dividing surface between the reactant and the product states. In the spirit of classical theory of Kohen and Tannor[25] we have recently formulated a quantum phase space function approach to reactive flux theory to derive a transmission coefficient in the intermediate to strong damping regime[19]. The object of the present paper is threefold: (i) to extend the treatment to numerical simulation for calculation of time-dependent transmission coefficient (ii) to analyze the Kramers' turnover, the T^2 enhancement of the rate at low temperature and some related features of temporal behaviour of the time-dependent transmission coefficient over a wide range of friction, noise correlation and temperature down to vacuum limit and (iii) to confirm the validity of our analytical result[19] in the spatial diffusion limited regime.

The present scheme of simulation is based on our recently proposed c-number Langevin equation[15,16,17,18,19] coupled to a set of quantum dispersion equations which take care of quantum corrections order by order. In what follows we make use of these equations to follow the evolution of an ensemble of c-number trajectories starting at the top of the barrier and sampling only the activated events and recrossing according to classical numerical reactive flux formulation of Straub and Berne[27,28,29].

The outlay of the paper is as follows: we first give an outline of c-number Langevin equation in Sec.II followed by a discussion on the method of numerical simulation for calculation of transmission coefficient using c-number reactive flux formalism in Sec.III. The numerical results are compared with those of others and discussed in Sec.IV. The paper is concluded in Sec.V.

II. A BRIEF OUTLINE OF C-NUMBER LANGEVIN EQUATION AND THE COUPLED QUANTUM DISPERSION EQUATIONS.

To start with we consider a particle coupled to a medium consisting of a set of harmonic oscillators with frequency ω_i. This is described by the following Hamiltonian.

$$H = \frac{\hat{p}^2}{2} + V(\hat{q}) + \sum_j \left\{ \frac{\hat{p}_j^2}{2} + \frac{1}{2}\kappa_j(\hat{q}_j - \hat{q})^2 \right\} \tag{1}$$

* Email address: pcdsr@mahendra.iacs.res.in

Here the masses of the particle and the reservoir oscillators have been taken to be unity. $\hat{q}$ and $\hat{p}$ are the coordinate and momentum operators of the particle, respectively and the set $\{\hat{q}_j, \hat{p}_j\}$ is the set of co-ordinate and momentum operators for the reservoir oscillators linearly coupled to the system through coupling constant κ_j. $V(\hat{q})$ denotes the external potential field which, in general, is nonlinear. The coordinate and momentum operators follow the usual commutation relations $[\hat{q}, \hat{p}] = i\hbar$ and $[\hat{q}_i, \hat{p}_j] = i\hbar\delta_{ij}$.

Eliminating the reservoir degrees of freedom in the usual way we obtain the operator Langevin equation for the particle

$$\ddot{\hat{q}}(t) + \int_0^t dt' \gamma(t-t')\dot{\hat{q}}(t') + V'(\hat{q}) = \hat{F}(t) \tag{2}$$

where the noise operator $\hat{F}(t)$ and the memory kernel $\gamma(t)$ are given by

$$\hat{F}(t) = \sum_j \left[\{\hat{q}_j(0) - \hat{q}(0)\}\kappa_j \cos\omega_j t + \hat{p}_j(0)\kappa_j^{1/2} \sin\omega_j t\right] \tag{3}$$

and

$$\gamma(t) = \sum_j \kappa_j \cos\omega_j t$$

or in the continuum limit

$$\gamma(t) = \int_0^\infty \kappa(\omega)\rho(\omega)\cos\omega t \; d\omega \tag{4}$$

$\rho(\omega)$ represents the density of the reservoir modes.

Eq.(2) is an exact operator Langevin equation for which the noise properties of $\hat{F}(t)$ can be defined using a suitable canonical initial distribution of bath co-ordinates and momenta. In what follows we proceed from this equation to derive a Langevin equation in c-numbers. The first step towards this goal is to carry out the *quantum mechanical average* of Eq.(2).

$$\langle\ddot{\hat{q}}(t)\rangle + \int_0^t dt' \gamma(t-t')\langle\dot{\hat{q}}(t')\rangle + \langle V'(\hat{q})\rangle = \langle\hat{F}(t)\rangle \tag{5}$$

where the average $\langle....\rangle$ is taken over the initial product separable quantum states of the particle and the bath oscillators at $t = 0$, $|\phi\rangle\{|\alpha_1\rangle|\alpha_2\rangle.....|\alpha_N\rangle\}$. Here $|\phi\rangle$ denotes any arbitrary initial state of the particle and $|\alpha_i\rangle$ corresponds to the initial coherent state of the i-th bath oscillator. $|\alpha_i\rangle$ is given by $|\alpha_i\rangle = \exp(-|\alpha_i|^2/2)\sum_{n_i=0}^{\infty}(\alpha_i^{n_i}/\sqrt{n_i!})|n_i\rangle$, α_i being expressed in terms of the mean values of the co-ordinate and momentum of the i-th oscillator, $\langle\hat{q}_i(0)\rangle = (\sqrt{\hbar}/2\omega_i)(\alpha_i + \alpha_i^\star)$ and $\langle\hat{p}_i(0)\rangle = i\sqrt{\hbar\omega_i/2}\;(\alpha_i^\star - \alpha_i)$, respectively. Now $\langle\hat{F}(t)\rangle$ is a classical-like noise term which, in general, is a nonzero number because of the quantum mechanical averaging over the co-ordinate and momentum operators of the bath oscillators with respect to initial coherent states and arbitrary initial state of the particle and is given by

$$\langle\hat{F}(t)\rangle = \sum_j \left[\{\langle\hat{q}_j(0)\rangle - \langle\hat{q}(0)\rangle\}\kappa_j \cos\omega_j t + \langle\hat{p}_j(0)\rangle\kappa_j^{1/2} \sin\omega_j t\right] \tag{6}$$

Now the operator Langevin equation can be written as

$$\langle\ddot{\hat{q}}\rangle + \int_0^t dt' \; \gamma(t-t')\langle\dot{\hat{q}}(t')\rangle + \langle V'(\hat{q})\rangle = f(t) \tag{7}$$

where $\langle\hat{F}(t)\rangle = f(t)$, denotes the quantum mechanical mean value.

We now turn to the *ensemble averaging*. To realize $f(t)$ as an effective c-number noise we now assume that the momentum $\langle\hat{p}_j(0)\rangle$ and the co-ordinate $\langle\hat{q}_j(0)\rangle - \langle\hat{q}(0)\rangle$ of the bath oscillators are distributed according to a canonical thermal Wigner distribution for shifted harmonic oscillator[37] as,

$$\mathcal{P}_j = \mathcal{N} \exp\left\{ -\frac{[\langle \hat{p}_j(0)\rangle^2 + \kappa_j \{\langle \hat{q}_j(0)\rangle - \langle \hat{q}(0)\rangle\}^2]}{2\hbar\omega_j \left(\bar{n}_j + \frac{1}{2}\right)} \right\} \tag{8}$$

so that for any quantum mean value $\mathcal{O}_j(\langle \hat{p}_j(0)\rangle, \{\langle \hat{q}_j(0)\rangle - \langle \hat{q}(0)\rangle\})$, the statistical average $\langle ....\rangle_s$ is

$$\langle \mathcal{O}_j \rangle_s = \int \mathcal{O}_j \; \mathcal{P}_j \; d\langle \hat{p}_j(0)\rangle \; d\{\langle \hat{q}_j(0)\rangle - \langle \hat{q}(0)\rangle\} \tag{9}$$

Here $\bar{n}_j$ indicates the average thermal photon number of the j-th oscillator at temperature T and is given by Bose-Einstein distribution $\bar{n}_j = 1/[\exp(\hbar\omega_j/kT) - 1]$ and $\mathcal{N}$ is the normalization constant.

The distribution Eq.(8) and the definition of the statistical average over quantum mechanical mean values Eq.(9) imply that $f(t)$ must satisfy

$$\langle f(t)\rangle_s = 0 \tag{10}$$

and

$$\langle f(t) f(t')\rangle_s = \frac{1}{2} \sum_j \kappa_j \; \hbar\omega_j \left(\coth \frac{\hbar\omega_j}{2kT}\right) \cos\omega_j(t - t')$$

or in the continuum limit

$$\begin{aligned} \langle f(t) f(t')\rangle_s &= \frac{1}{2} \int_0^\infty d\omega \; \kappa(\omega) \; \rho(\omega) \; \hbar\omega \left(\coth \frac{\hbar\omega}{2kT}\right) \cos\omega(t - t') \\ &\equiv c(t - t') \end{aligned} \tag{11}$$

That is, c-number noise $f(t)$ is such that it is zero-centered and satisfies the standard fluctuation-dissipation relation as known in the literature. For other details we refer to [16-20].

We now add the force term $V'(\langle \hat{q}\rangle)$ on both sides of the Eq.(7) and rearrange it to obtain

$$\ddot{q}(t) + V'(q) + \int_0^t dt' \; \gamma(t - t') \; \dot{q}(t') = f(t) + Q(t) \tag{12}$$

where we put $\langle \hat{q}(t)\rangle = q(t)$ and $\langle \dot{\hat{q}}(t)\rangle = p(t)$; $q(t)$ and $p(t)$ being quantum mechanical mean values and also

$$Q(t) = V'(q) - \langle V'(\hat{q})\rangle \tag{13}$$

represents the quantum correction to classical potential.

Eq.(12) which is based on the ansatz Eq.(8), is governed by a c-number noise $f(t)$ due to the heat bath, characterized by Eq.(10), Eq.(11) and a quantum correction term $Q(t)$ characteristic of the nonlinearity of the potential. The canonical thermal Wigner distribution - the ansatz Eq.(8) is always positive definite. It goes over to a pure state distribution for the ground state of shifted harmonic oscillator in the vacuum limit, i.e. , at $T = 0$ which is again a well-behaved[37] distribution. The quantum nature of the dynamics thus arises from two sources. The first one is due to the quantum heat bath. The second one is because of nonlinearity of the system potential as embedded in $Q(t)$ of Eq.(15). To make the description complete for practical calculation one has to have a recipe for calculation of $Q(t)$[15,16,17,18,19,30,31]. For the present purpose we summarize it as follows:

Referring to the quantum mechanics of the system in the Heisenberg picture one may write,

$$\begin{aligned} \hat{q}(t) &= \langle \hat{q}(t)\rangle + \delta\hat{q}(t) \\ \hat{p}(t) &= \langle \hat{p}(t)\rangle + \delta\hat{p}(t) \end{aligned} \tag{14}$$

$\delta\hat{q}(t)$ and $\delta\hat{p}(t)$ are the operators signifying quantum corrections around the corresponding quantum mechanical mean values q and p. By construction $\langle\delta\hat{q}\rangle = \langle\delta\hat{p}\rangle = 0$ and $[\delta\hat{q}, \delta\hat{p}] = i\hbar$. Using Eq.(14) in $\langle V'(\hat{q})\rangle$ and a Taylor series expansion around $\langle\hat{q}\rangle$ it is possible to express $Q(t)$ as

$$Q(t) = -\sum_{n\geq 2} \frac{1}{n!} V^{(n+1)}(q)\langle\delta\hat{q}^n(t)\rangle \tag{15}$$

Here $V^{(n)}(q)$ is the n-th derivative of the potential $V(q)$. To second order $Q(t)$ is given by $Q(t) = -\frac{1}{2}V'''(q)\langle\delta\hat{q}^2(t)\rangle$ where $q(t)$ and $\langle\delta\hat{q}^2(t)\rangle$ can be obtained as explicit functions of time by solving following set of approximate coupled equations Eq.(16) to Eq.(18) together with Eq.(12)

$$\frac{d}{dt}\langle\delta\hat{q}^2\rangle = \langle\delta\hat{q}\delta\hat{p} + \delta\hat{p}\delta\hat{q}\rangle \tag{16}$$

$$\frac{d}{dt}\langle\delta\hat{q}\delta\hat{p} + \delta\hat{p}\delta\hat{q}\rangle = 2\langle\delta\hat{p}^2\rangle - 2V''(q)\langle\delta\hat{q}^2\rangle \tag{17}$$

$$\frac{d}{dt}\langle\delta\hat{p}^2\rangle = -V''(q)\langle\delta\hat{q}\delta\hat{p} + \delta\hat{p}\delta\hat{q}\rangle \tag{18}$$

While the above set of equations provide analytic solutions containing lowest order quantum corrections, the successive improvement of $Q(t)$ can be achieved by incorporating higher order contribution due to the potential $V(q)$ and the dissipation effects on the quantum correction terms. In Appendix A we have derived the equations for quantum corrections upto fourth order[30] as employed in the present numerical scheme. Under very special circumstances, it has been possible to include quantum effects to all orders[18,31]. The appearance of $Q(t)$ as a quantum correction term due to nonlinearity of the system potential and dependence of friction on frequency make the c-number Langevin equation (Eq.(12)) distinct from the earlier equations of Schmid and Eckern *et al*[39,40]. The approach has been recently utilized by us to derive the quantum analogues[15,16,17,18] of classical Kramers, Smoluchowski and diffusion equations with probability distribution functions of c-number variables. An important success of the scheme is that these equations of motion for probability distribution functions do not contain derivatives of the distribution functions higher than second for nonlinear potentials ensuring positive definiteness of the distribution functions. This is in contrast to usual situations[38] where one encounters higher derivatives of Wigner, Glauber-Sudarshan distribution functions for nonlinear potential and the positive definiteness is never guaranteed. More recently the classical Kohen-Tannor formalism of reactive flux has been extended to quantum domain[19]. In what follows we present a numerical simulation of reactive flux using c-number Langevin dynamics.

III. NUMERICAL SIMULATION

The numerical solution of Eq.(12), along with Eqs.(A1) to Eq.(A3) is performed according to the following main steps.

We first briefly outline the method of generation of c-number noise. Eq.(11) is the fluctuation-dissipation relation and is the key element for generation of c-number noise. $\langle f(t)f(t')\rangle_s$ is correlation function which is classical in form but quantum mechanical in content. We now show that c-number noise $f(t)$ is generated as a superposition of several Ornstein-Ulhenbeck noise processes. It may be noted that in the continuum limit $c(t-t')$ is given by

$$c(t-t') = \frac{1}{2}\int_0^\infty d\omega\ \kappa(\omega)\ \rho(\omega)\ \hbar\omega\left(\coth\frac{\hbar\omega}{2kT}\right)\cos\omega(t-t') \tag{19}$$

In determining the evolution of stochastic dynamics governed by Eq.(12) it is essential to know a priori the form of $\rho(\omega)\kappa(\omega)$. We assume a Lorentzian distribution of modes so that

$$\kappa(\omega)\rho(\omega) = \frac{2}{\pi}\left(\frac{\Gamma}{1+\omega^2\ \tau_c^2}\right) \tag{20}$$

where Γ and τ_c are the dissipation in the Markovian limit and correlation time, respectively. Eq.(20) when used in Eq.(4) in the continuum limit yields an exponential memory kernel $\gamma(t) = (\Gamma/\tau_c)e^{-t/\tau_c}$. For a given set of parameters

Γ and τ_c along with temperature T, we first numerically evaluate the integral (19) as a function of time. In the next step we numerically fit the correlation function with a superposition of several exponentials,

$$c(t-t') = \sum_i \frac{D_i}{\tau_i} \exp\left(\frac{-|t-t'|}{\tau_i}\right), \qquad i = 1, 2, 3... \tag{21}$$

The set D_i and τ_i the constant parameters are thus known. In Fig.1 we compare the correlation $c(t)$ determined from the relation (19) with the superposition (21) for three different temperatures at $kT = 1.0$, 0.5 and 0.1 for $\Gamma = 1.0$ and $\tau_c = 3.0$. The numerical agreement between the two sets of curves based on Eq.(19) and Eq.(21) suggests that one may generate a set of exponentially correlated color noise variables η_i according to

$$\dot{\eta}_i = -\frac{\eta_i}{\tau_i} + \frac{1}{\tau_i}\,\xi_i(t) \tag{22}$$

where

$$\langle \xi_i(t) \rangle = 0 \quad and \quad \langle \xi_i(0)\xi_j(\tau) \rangle = 2D_i\,\delta_{ij}\,\delta(\tau) \qquad (i = 1, 2, 3....) \tag{23}$$

in which $\xi_i(t)$ is a Gaussian white noise obeying Eq.(23), τ_i, D_i being determined from numerical fit. The noise η_i is thus an Ornstein-Ulhenbeck process with properties.

$$\langle \eta_i(t) \rangle = 0 \quad and \quad \langle \eta_i(t)\eta_j(t') \rangle = \delta_{ij}\,\frac{D_i}{\tau_i} \exp\left(\frac{-|t-t'|}{\tau_i}\right) \qquad (i = 1, 2, 3....) \tag{24}$$

Clearly τ_i and D_i are the correlation time and strength of the color noise variable η_i. The c-number noise $f(t)$ due to heat bath is therefore given by

$$f(t) = \sum_{i=1}^{n} \eta_i \tag{25}$$

Having obtained the scheme for generation of c-number noise $f(t)$ we now proceed to solve the stochastic differential equations.

In order to solve the c-number Langevin equation Eq.(12) we may write it in the equivalent form[29,32,33]

$$\begin{aligned}
\dot{q} &= p \\
\dot{p} &= -V'(q) + Q(t) + \sum_i \eta_i(t) + z \\
\dot{z} &= -\Gamma\frac{p}{\tau_c} - \frac{z}{\tau_c} \\
\dot{\eta}_i &= -\frac{\eta_i}{\tau_i} + \frac{1}{\tau_i}\,\xi_i(t)
\end{aligned} \tag{26}$$

The integration of the above set of equations[26,29] is carried out using the second order Heun's algorithm. A very small time step size, 0.001, has been used.

The above set of equations differ from the corresponding classical equations in two ways. First, the noise correlation of c-number heat bath variables $f(t)$ are quantum mechanical in character which is reflected in D_i and τ_i. Second, the knowledge of $Q(t)$ requires the quantum correction equations given in the Appendix A which provides quantum dispersion about the quantum mechanical mean values q and p of the system. It is thus essential to take care of these contributions. A simple way to achieve this is to solve the equations Eq.(A1) to Eq.(A3) in the Appendix A for $\langle \delta\hat{q}^n(t) \rangle$ by starting with N-particles (say, around 5000) all of them above the barrier top at $q = 0$, half with a positive velocity distributed according to velocity distribution[19] $p\,\exp\left(\frac{-p^2}{2\hbar\omega_0(\overline{n}_0+1/2)}\right)$ and the other half with the same distribution with negative velocities, initial values of dispersion being set as $\langle \delta\hat{q}^2(t) \rangle_{t=0} = 0.5$, $\langle \delta\hat{q}\,\delta\hat{p} + \delta\hat{p}\,\delta\hat{q} \rangle_{t=0} = 1.0$, $\langle \delta\hat{p}^2(t) \rangle_{t=0} = 0.5$ and with others set as zero. The width of the distribution is the same as that for Eq.(8) where ω_j is

replaced by ω_0 corresponding to the reactant harmonic well which is in equilibrium with the bath. We take the time averaged contribution of the quantum corrections upto $1/\Gamma$ time for each trajectory to solve the Langevin equation Eq.(26) for N-particles. The time dependent transmission coefficient is calculated from these sets of simulated data by calculating

$$\kappa(t) = \frac{N_+(t)}{N_+(0)} - \frac{N_-(t)}{N_-(0)} \tag{27}$$

where $N_+(t)$ and $N_-(t)$ are the particles that started with positive velocities and negative velocities, respectively and at time t are in or over the right hand well (i.e. the particles for which the quantum mean value $q(t) > 0$).

IV. RESULTS AND DISCUSSIONS

We now consider the potential of the form $V(q) = a\ q^4 - b\ q^2$, where a and b are the two parameters. The other three input parameters for our calculations are temperature T, strength of noise correlation Γ and correlation time τ_c. For the present purpose we fix $a = 0.001$ and $b = 0.5$ for the entire calculation except those for Fig.3 and Fig.8. In order to ensure the stability of the algorithm we have kept $\Delta t/\tau_c << 1$ where Δt is the integration time step size. Fig.2 exhibits the temporal variation of classical transmission coefficient (dotted line) and transmission coefficient calculated by present method (solid line) for two typical different parameter regimes (a) $\Gamma = 3.0$ and (b) $\Gamma = 5.0$ for $kT = 0.5$, $\tau_c = 3.0$ to illustrate the differential behaviour of the classical[26] and quantum effects. In the both cases one observes significant increase in transmission coefficient due to quantum contribution over and above the magnitude of classical transmission coefficient. In order to extract out the contribution of quantum correction due to nonlinearity of the system potential $Q(t)$ we exhibit in Fig.3 the time dependent transmission coefficient for the parameter set $a = 0.005$, $b = 0.5$, $kT = 0.025$, $\Gamma = 1.0$ and $\tau_c = 1.0$ with (dotted line) and without (solid line) second order quantum corrections. It is observed that the quantum corrections due to nonlinearity affects the stationary values more than the transient ones.

In order to check the workability of the method we now compare in Fig.4 the temporal variation of numerical (dotted line) and analytical[19] (solid line) transmission coefficient at $kT = 1.0$ for two different parameter regimes characteristic of adiabatic regime (a) $\Gamma = 2.0$, $\tau_c = 5.0$ (b) $\Gamma = 4.0$, $\tau_c = 8.0$ and caging regime (c) $\Gamma = 90.0$, $\tau_c = 10.0$, the two regimes being differentiated according to ω_b, Γ and τ_c; adiabatic ($\omega_b^2 - \Gamma/\tau_c > 0$); caging (($\omega_b^2 - \Gamma/\tau_c < 0$), ω_b refers to the barrier frequency). We observe that while in the adiabatic regime the agreement is excellent the numerical transmission coefficients tend to settle down around zero relatively earlier compared to analytical one in the caging regime; the numerically calculated phase of oscillation, however, corresponds correctly to its analytical counterpart. Keeping in view of the fact that the analytical results are based on a phase space function approach which is independent of the method of numerical simulation, we believe that the agreement is quite satisfactory in both adiabatic and caging regimes which ensures the validity of the numerical procedure as followed in the present treatment.

In Fig.5 we show the typical simulation results over a range of dissipation parameters Γ from 0.01 to 8.0 for $\tau_c = 1.0$ and $kT = 1.0$. For a low value of Γ, e.g., 0.01 simulation result remains at a high value for some period to drop rather suddenly and to settle finally in an oscillatory way to a low asymptotic value. The behaviour is almost qualitatively same as its classical counterpart as shown by Sancho, Romero and Lindenberg[26]. The long temporal oscillation of transmission coefficient calculated by the c-number method is typical for very low dissipation regime. As dissipation increases to 0.5 the temporal variation of $\kappa(t)$ becomes monotonic and $\kappa(t)$ settles down much earlier at a much higher asymptotic value. For $\Gamma = 1.0$ to 8.0 the transmission coefficient decreases rather significantly. The oscillations at short times for $\Gamma = 5.0$ and 8.0 are due to usual transient recrossings.

The variation of asymptotic transmission coefficient with dissipation parameter Γ in Fig.5 illustrates the well known turnover phenomenon. In Figs.6-8 we analyze this aspect in greater detail. To this end we show in Fig.6 how the asymptotic transmission coefficient as a function of dissipation constant Γ calculated (classical) earlier by Lindenberg *et al*[26] follows closely to that of ours at relatively high temperature $kT = 3.0$ for $\tau_c = 3.0$. The agreement between the two allows us to have a numerical check on the method and to ensure the validity of the result in the classical limit. The turnover problem was investigated earlier by Melnikov *et al*[34] and Pollak *et al*[35] to obtain correct analytical solution bridging the spatial diffusion and the energy diffusion regimes and that goes over to the limiting behaviour at high and low dissipation. To explore the quantum effects we study the turnover behaviour at various temperatures down to absolute zero as shown in Fig.7 for $\tau_c = 3.0$. As the temperature is lowered the maximum at which the turnover occurs shifts to the left and the damping regime that corresponds to classical energy diffusion, i.e., in the low damping regime becomes exponentially small as one approaches to absolute zero. It is fully consistent with the earlier observation[9] made on this issue.

To check the validity of the numerical results on quantum turnover in a more quantitative way we have further compared in Fig.8 our results (solid lines) with full quantum results (dotted lines) of Topaler and Makri[13] (Fig. 9a-b of Ref.12) for two different scaled temperatures $kT = 1.744(200K)$ and $kT = 2.617(300K)$ for a double well potential with $a = 0.0024$ and $b = 0.5$ in the Ohmic regime. It is immediately apparent from Fig.8 that the transmission coefficients calculated by simulation of the c-number Langevin equation with fourth order quantum corrections compared satisfactorily with the full quantum results based on path integral Monte Carlo method of Topaler and Makri[13].

In Fig.9 we plot the temporal behaviour of transmission coefficient $\kappa(t)$ for different temperatures for $\Gamma = 1.0$ and $\tau_c = 1.0$. It is observed that $\kappa(t)$ quickly settles after a fast fall and the asymptotic values of the transmission coefficient converge to a temperature independent value as the temperature is increased from $kT = 0.0$ to $kT = 5.0$. Fig.10 exhibits this variation of asymptotic value of transmission coefficient (dotted line) explicitly as a function of temperature and a comparison with analytical[19] results (solid line) for $\Gamma = 2.0$ and $\tau_c = 5.0$. The agreement is found to be excellent. In order to analyze the temperature dependence of the transmission coefficient at low temperature and compare with earlier results[36], the numerical result (solid line) is fitted against a function of the form (dotted line) $A\exp(B/T^2)$, in the inset of Fig.10, where A and B are fitting constants. The well known T^2 enhancement of the quantum rate is observed upto a low temperature beyond which the fitting curve tends to diverge rapidly as $kT \to 0$. This divergence of the rate at very low temperature had been noted earlier in the analytical result of Grabert *et at*[36]. In the present calculation, however the transmission coefficient reaches its maximum finite value within unity and its validity is retained even in the vacuum limit. Thus in contrast to classical transmission coefficient the temperature dependence remains a hallmark of quantum signature of the transmission coefficient. In Fig.11 we show the temporal behaviour of the transmission coefficient for several values of the noise correlation time τ_c for $kT = 1.0$ $\Gamma = 1.0$. The asymptotic transmission coefficient increases as expected from theoretical point of view.

V. CONCLUSION

The primary aim of this paper is to extend our recent treatment of c-number Langevin equation to calculate numerically the time dependent transmission coefficient within the framework of reactive flux formalism. Since the quantum dynamics is amenable to a theoretical description in terms of ordinary coupled equations which are classical looking in form it is possible to employ the numerical simulation scheme of Straub and Berne in a quite straight forward way for calculation of transmission coefficient. There are two special advantages in the procedure. First, since we are concerned with the dynamics of quantum mechanical mean values coupled to quantum correction equations, we need not calculate higher moments $\langle\hat{q}^2\rangle$ or $\langle\hat{p}^2\rangle$ etc in any stage of calculations. This makes the calculation simpler. Secondly, the treatment can be readily used to calculate the dynamics even in the vacuum limit, i.e., $kT \to 0$, where it is expected that because of the oscillating nature of the real time propagator in path integral method Monte Carlo schemes pose very serious problems from applicational point of view. We have extended the classical simulation procedure to a quantum domain taking into consideration of the quantum effects in two different ways. The quantum effects enter through the correlation function of the c-number noise variables of the heat bath and furthermore, through nonlinearity of the system potential which is entangled with quantum dispersion around the quantum mechanical mean values of the system operators. We summarize the main results as follows:

(i) The present method is a direct extension of classical simulation method of Straub and Berne to quantum domain for calculation of transmission coefficient within a c-number version of reactive flux formalism. Although the quantum effects due to heat bath can be taken into account in terms of noise correlation expressed in quantum fluctuation-dissipation relation, the quantum dispersion around the quantum mean values of the system operators are to be calculated order by order. Notwithstanding the latter consideration the method is efficient when compared to full quantum mechanical calculation as demonstrated in the present simulation.

(ii) We have calculated the time dependent transmission coefficient for a double well potential over a wide range of friction and temperature and shown that our numerical simulation results on turnover phenomena, low temperature enhancement of quantum rate and other features agree satisfactorily with those calculated analytically/otherwise using phase space function and other approaches. The differential behaviour of the classical and transmission coefficients calculated by the classical and present c-number method has been analyzed in detail. The procedure is equipped to deal with arbitrary noise correlation, strength of dissipation and temperature down to vacuum limit, i.e., $kT \to 0$.

(iii) The present approach is independent of path integral approaches and is based on canonical quantization and Wigner quasiclassical phase space function and takes into account of the quantum effects upto a significant degree of accuracy. This procedure simply depends on the solutions of coupled ordinary differential equations rather than the multi-dimensional path integral Monte Carlo techniques and is therefore complementary to these approaches, much simple to handle and corresponds more closely to classical procedure.

Acknowledgement We are thankful to S. K. Banik for discussions. The authors are indebted to the Council of

Scientific and Industrial Research for partial financial support under Grant No. 01/(1740)/02/EMR-II.

APPENDIX A

Evolution Equations For Higher-Order Quantum Corrections For Anharmonic Potential

The equations upto fourth order for quantum corrections (corresponding to the contribution of anharmonicity of the potential) with dissipative effects taking into consideration of Lorentzian density of reservoir modes of the form Eq.(20), in the limit τ_c very small, are listed below.
Equations for the second order are:

$$\begin{aligned}
\frac{d}{dt}\langle\delta\hat{q}^2\rangle &= \langle\delta\hat{q}\delta\hat{p}+\delta\hat{p}\delta\hat{q}\rangle,\\
\frac{d}{dt}\langle\delta\hat{p}^2\rangle &= -2\Gamma\langle\delta\hat{p}^2\rangle - V''\langle\delta\hat{q}\delta\hat{p}+\delta\hat{p}\delta\hat{q}\rangle - V'''\langle\delta\hat{q}\delta\hat{p}\delta\hat{q}\rangle,\\
\frac{d}{dt}\langle\delta\hat{q}\delta\hat{p}+\delta\hat{p}\delta\hat{q}\rangle &= -\Gamma\langle\delta\hat{q}\delta\hat{p}+\delta\hat{p}\delta\hat{q}\rangle 2\langle\delta\hat{p}^2\rangle - 2V''\langle\delta\hat{q}^2\rangle - V'''\langle\delta\hat{q}^3\rangle,
\end{aligned} \tag{A1}$$

Those for the third order are:

$$\begin{aligned}
\frac{d}{dt}\langle\delta\hat{q}^3\rangle &= 3\langle\delta\hat{q}\delta\hat{p}\delta\hat{q}\rangle,\\
\frac{d}{dt}\langle\delta\hat{p}^3\rangle &= -3\Gamma\langle\delta\hat{p}^3\rangle - 3V''\langle\delta\hat{p}\delta\hat{q}\delta\hat{p}\rangle + V'''\left(\frac{3}{2}\langle\delta\hat{q}^2\rangle\langle\delta\hat{p}^2\rangle - \frac{3}{2}\langle\delta\hat{p}\delta\hat{q}^2\delta\hat{p}\rangle + \hbar^2\right),\\
\frac{d}{dt}\langle\delta\hat{q}\delta\hat{p}\delta\hat{q}\rangle &= -\Gamma\langle\delta\hat{q}\delta\hat{p}\delta\hat{q}\rangle + 2\langle\delta\hat{p}\delta\hat{q}\delta\hat{p}\rangle - V''\langle\delta\hat{q}^3\rangle - \frac{V'''}{2}\left(\langle\delta\hat{q}^4\rangle - \langle\delta\hat{q}^2\rangle^2\right),\\
\frac{d}{dt}\langle\delta\hat{p}\delta\hat{q}\delta\hat{p}\rangle &= -2\Gamma\langle\delta\hat{p}\delta\hat{q}\delta\hat{p}\rangle + \langle\delta\hat{p}^3\rangle - 2V''\langle\delta\hat{q}\delta\hat{p}\delta\hat{q}\rangle\\
&+ \frac{V'''}{2}\left(\langle\delta\hat{q}^2\rangle\langle\delta\hat{q}\delta\hat{p}+\delta\hat{p}\delta\hat{q}\rangle - \langle\delta\hat{q}^3\delta\hat{p}+\delta\hat{p}\delta\hat{q}^3\rangle\right),
\end{aligned} \tag{A2}$$

And lastly, the fourth order equations are:

$$\begin{aligned}
\frac{d}{dt}\langle\delta\hat{q}^4\rangle &= 2\langle\delta\hat{q}^3\delta\hat{p}+\delta\hat{p}\delta\hat{q}^3\rangle,\\
\frac{d}{dt}\langle\delta\hat{p}^4\rangle &= -4\Gamma\langle\delta\hat{p}^4\rangle - 2V''\langle\delta\hat{q}\delta\hat{p}^3+\delta\hat{p}^3\delta\hat{q}\rangle + 2V'''\langle\delta\hat{q}^2\rangle\langle\delta\hat{p}^3\rangle,\\
\frac{d}{dt}\langle\delta\hat{q}^3\delta\hat{p}+\delta\hat{p}\delta\hat{q}^3\rangle &= -\Gamma\langle\delta\hat{q}^3\delta\hat{p}+\delta\hat{p}\delta\hat{q}^3\rangle - 2V''\langle\delta\hat{q}^4\rangle - 3\hbar^2 + 6\langle\delta\hat{p}\delta\hat{q}^2\delta\hat{p}\rangle\\
&+ V'''\langle\delta\hat{q}^2\rangle\langle\delta\hat{q}^3\rangle,\\
\frac{d}{dt}\langle\delta\hat{q}\delta\hat{p}^3+\delta\hat{p}^3\delta\hat{q}\rangle &= -3\Gamma\langle\delta\hat{q}\delta\hat{p}^3+\delta\hat{p}^3\delta\hat{q}\rangle + 2\langle\delta\hat{p}^4\rangle + 3V''(\hbar^2 - 2\langle\delta\hat{p}\delta\hat{q}^2\delta\hat{p}\rangle)\\
&+ 3V'''\langle\delta\hat{q}^2\rangle\langle\delta\hat{p}\delta\hat{q}\delta\hat{p}\rangle,\\
\frac{d}{dt}\langle\delta\hat{p}\delta\hat{q}^2\delta\hat{p}\rangle &= -2\Gamma\langle\delta\hat{p}\delta\hat{q}^2\delta\hat{p}\rangle - V''\langle\delta\hat{q}^3\delta\hat{p}+\delta\hat{p}\delta\hat{q}^3\rangle + \langle\delta\hat{p}^3\delta\hat{q}+\delta\hat{q}\delta\hat{p}^3\rangle\\
&+ V'''\langle\delta\hat{q}^2\rangle\langle\delta\hat{q}\delta\hat{p}\delta\hat{q}\rangle.
\end{aligned} \tag{A3}$$

The derivatives of $V(q)$, i.e., V'' or V''' etc. in the above expressions are functions of q the dynamics of which is given by Eq.(12).

---

[1] H.A. Kramers, Physica **7**, 284 (1940).

[2] R.F. Grote and J.T. Hynes, J. Chem. Phys. **73**, 2715 (1980).
[3] B. Carmeli and A. Nitzan, J. Chem. Phys. **79**, 393 (1983).
[4] J.S. Langer, Ann. Phys. (N.Y.) **54**, 258 (1969).
[5] A.M. Berezhkovskii, E. Pollak and V. Yu Zitserman, J. Chem. Phys. **97**, 2422 (1992).
[6] J. Ray Chaudhuri, B.C. Bag and D.S. Ray, J. Chem. Phys. **111**, 10852 (1999).
[7] U. Weiss, *Quantum Dissipative Systems*, (World Scientific, Singapore, 1999).
[8] J. T. Stockburger and H. Grabert, Phys. Rev. Lett. **88**, 170407 (2002)
[9] P. Hänggi, P. Talkner and M. Borkovec, Rev. Mod. Phys. **62**, 251 (1990).
[10] P.G. Wolynes, Phys. Rev. Lett. **47**, 968 (1981).
[11] W.H. Miller, J. Chem. Phys. **62**, 1899 (1975).
[12] A.O. Caldeira and A.J. Leggett, Phys. Rev. Lett. **46**, 211 (1981).
[13] M. Topaler and N. Makri, J. Chem. Phys. **101**, 7500 (1994) and References given therein.
[14] B.J. Berne and D. Thirumalai, Ann. Rev. Phys. Chem. **37**, 401 (1987); *Quantum Simulations of Condensed Matter Phenomena edited by J. D. Doll and Gubernatis* (World Scientific, Singapore, 1999).
[15] D. Banerjee, B.C. Bag, S.K. Banik and D.S. Ray, Phys. Rev. E **65**, 021109 (2002).
[16] S.K. Banik, B.C. Bag and D.S. Ray, Phys. Rev. E **65**, 051106 (2002).
[17] D. Banerjee, S.K. Banik, B.C. Bag, and D.S. Ray, Phys. Rev. E **66**, 051105 (2002).
[18] D. Banerjee, B.C. Bag, S.K. Banik and D.S. Ray, Physica A **318**, 6 (2003)
[19] D. Barik, S.K. Banik and D.S. Ray, J. Chem. Phys. **119**, 680 (2003)
[20] R.D. Astumian, Science **276**, 917 (1997); F. Julicher, A. Adjari and J. Prost, Rev. Mod. Phys. **69**, 1269 (1997); P. Reimann, Phys. Rep. **361**, 57 (2002).
[21] J.C. Keck, Adv. Chem. Phys. **13**, 85 (1967).
[22] R. Kapral, J. Chem. Phys. **56**, 1842 (1972).
[23] D. Chandler, J. Chem. Phys. **68**, 2969 (1978).
[24] K. Yamashita and W.H. Miller, J. Chem. Phys. **82**, 5475 (1985); J.W. Tromp and W.H. Miller, Faraday Discuss Chem. Soc. **84**, 441 (1987); W.H. Miller, S.D. Schwartz and J.W. Tromp, J. Chem. Phys. **79**, 4889 (1983).
[25] D.J. Tannor and D. Kohen, J. Chem. Phys. **100**, 4932 (1994); D. Kohen and D.J. Tannor, **103**, 6013 (1995); D. Kohen and D. J. Tannor, Adv. Chem. Phys. **111**, 219 (1999).
[26] J.M. Sancho, A.H. Romero and K. Lindenberg, J. Chem. Phys. **109**, 9888 (1998); K. Lindenberg, A.H. Romero and J.M. Sancho, Physica D **133**, 348 (1999).
[27] J.E. Straub and B.J. Berne, J. Chem. Phys. **83**, 1138 (1985)
[28] J.E. Straub, D.A. Hsu and B.J. Berne, J. Chem. Phys. **89**, 5788 (1985)
[29] J.E. Straub, M. Borkovec and B.J. Berne, J. Chem. Phys. **84**, 1788 (1986)
[30] B. Sundaram and P.W. Milonni, Phys. Rev. E **51**, 1971 (1995).
[31] A.K. Pattanayak and W.C. Schieve, Phys. Rev. E **50**, 3601 (1994).
[32] R. Zwanzig, J. Chem. Phys. **86**, 5801 (1987)
[33] J.E. Straub and B.J. Berne, J. Chem. Phys. **85**, 2999 (1986)
[34] V. I. Melnikov and S.V. Meshkov, J. Chem. Phys. **85**(2), 3271 (1986).
[35] I. Rips and E. Pollak, Phys. Rev. A **41**, 5366 (1990)
[36] P. Hanggi, H. Grabert, G. L. Ingold and U. Weiss, Phys. Rev. Lett. **55**, 761 (1985)
[37] M. Hillery, R. F. O'Connell, M. O. Scully and E. P. Wigner, Phys. Rep. **106**, 121 (1984)
[38] W. H. Louisell, *Quantum Statistical Properties of Radiation*, (J. Wiley, 1973)
[39] A. Schmid, J. Low. Temp. Phys. **49**, 609 (1982)
[40] U. Eckern, W. Lehr, A. Menzel-Dorwarth, F. Pelzer and A. Schmid, J. Stat. Phys. **59**, 885 (1990)

FIGURE CAPTIONS

Fig.1: Plot of correlation function $c(t)$ vs t as given by Eq.(19) (solid line) and Eq.(21) (dotted line) for the set of parameter values mentioned in the text.

Fig.2: A comparison of transmission coefficients (classical(dotted line); c-number method(solid line)) as function of time t is plotted for (a) $\Gamma = 3.0$ (b) $\Gamma = 5.0$ for the parameter set mentioned in the text.

Fig.3: The numerical transmission coefficient $\kappa(t)$ is plotted against time with (dotted line) and without (solid line) quantum correction $Q(t)$ for $a = 0.005$, $b = 0.5$, $\Gamma = 1.0$, $\tau_c = 1.0$ at $kT = 0.025$

Fig.4: Numerical transmission coefficient $\kappa(t)$ is plotted against time t and compared with c-number analytical[19] $\kappa(t)$ for adiabatic regime [(a) $\Gamma = 2.0, \tau_c = 5.0$, (b) $\Gamma = 4.0, \tau_c = 8.0$] and caging regime [$\Gamma = 90.0, \tau_c = 10.0$] for the parameter set mentioned in the text.

Fig.5: Transmission coefficient, $\kappa(t)$ is plotted against time for different values of Γ for the parameter set mentioned in the text.

Fig.6: A comparison of the turnover (plot of asymptotic κ vs Γ) calculated by Sancho, Romero and Lindenberg[26] (circle) with that by the present method (square) for the parameter set mentioned in the text.

Fig.7: Kramers' turnover (plot of asymptotic κ vs Γ) for different temperatures for the parameters set mentioned in the text for $kT = 0.0$ (downtriangle), $kT = 0.5$ (circle), $kT = 1.0$ (square) and $kT = 3.0$ (uptriangle).

Fig.8: A comparison of the Kramers' turnover (plot of assymptotic κ vs Γ) for two temperatures (a) $kT = 2.617(300K)$ and (b) $kT = 1.744(200K)$ between the present result (solid line) and full quantum result (dotted line) of Topaler and Makri (Fig.9a-b of ref.12) for the double well potential with $a = 0.0024$ and $b = 0.5$ in the Ohmic regime.

Fig.9: Transmission coefficient $\kappa(t)$ is plotted against time t for different values of temperature, $kT = 0.0$ (solid line), $kT = 0.5$ (dash dot dot line), $kT = 1.0$ (dash dot line), $kT = 2.0$ (dashed line) and $kT = 5.0$ (dotted line) for the set of parameters mentioned in the text.

Fig.10: Asymptotic transmission coefficient is plotted against temperature (dotted line: analytical[19], solid line: numerical) for the parameter set mentioned in the text. Inset: the same numerical curve (solid line) is plotted against a fitted curve (dotted) to exhibit T^2 enhancement of rate at low temperature.

Fig.11: Transmission coefficient $\kappa(t)$ is plotted against time for different values of τ_c for the parameter set mentioned in the text.

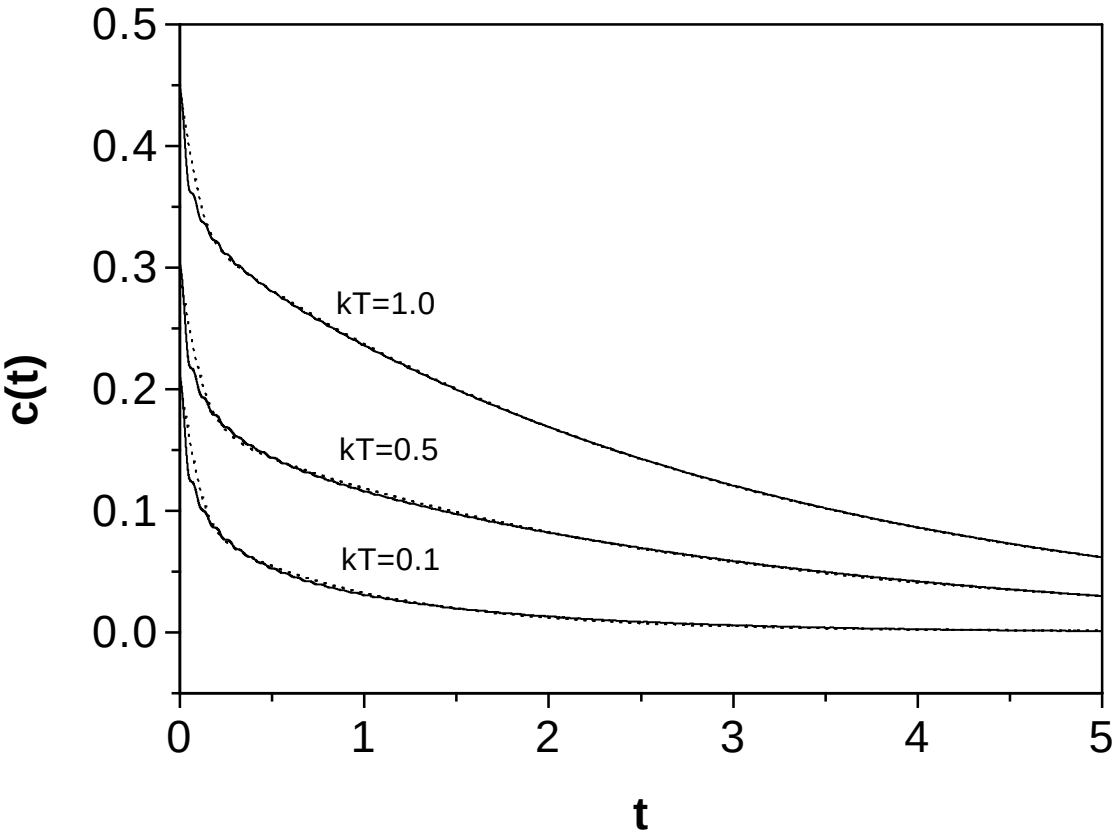

Fig.1

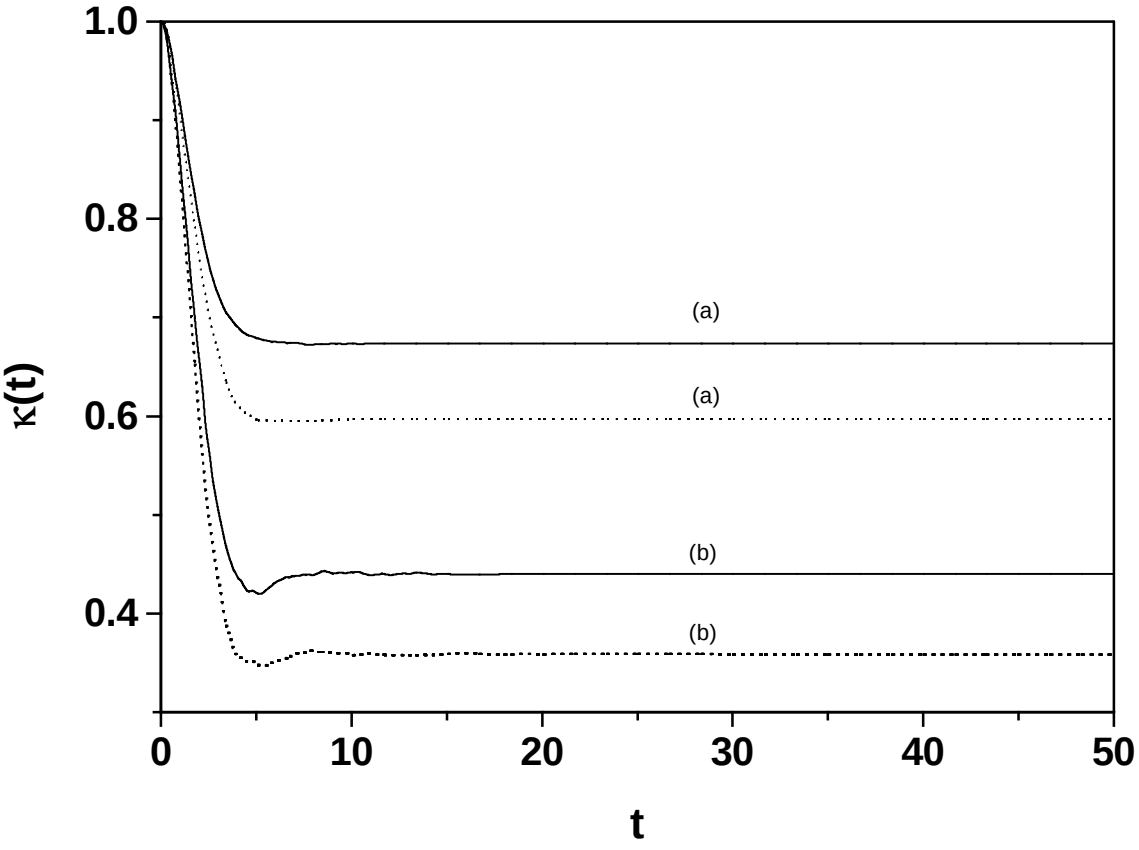

Fig.2

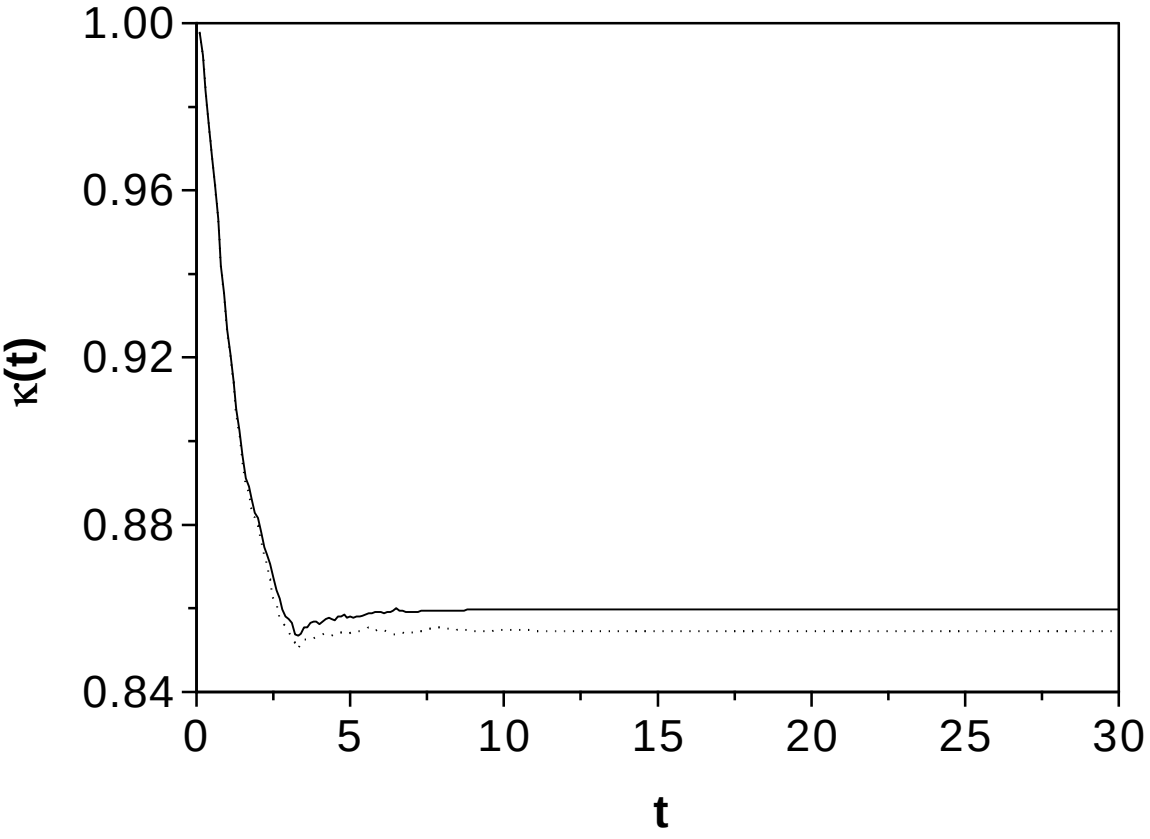

Fig.3

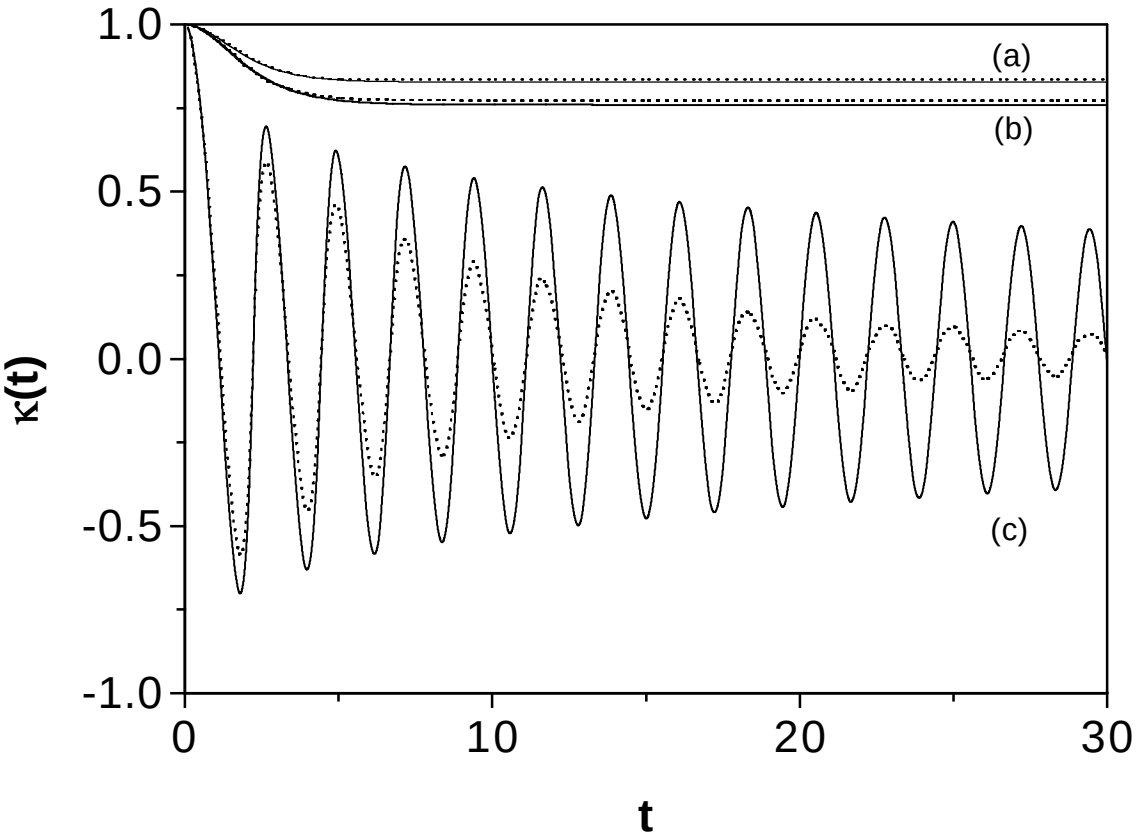

Fig.4

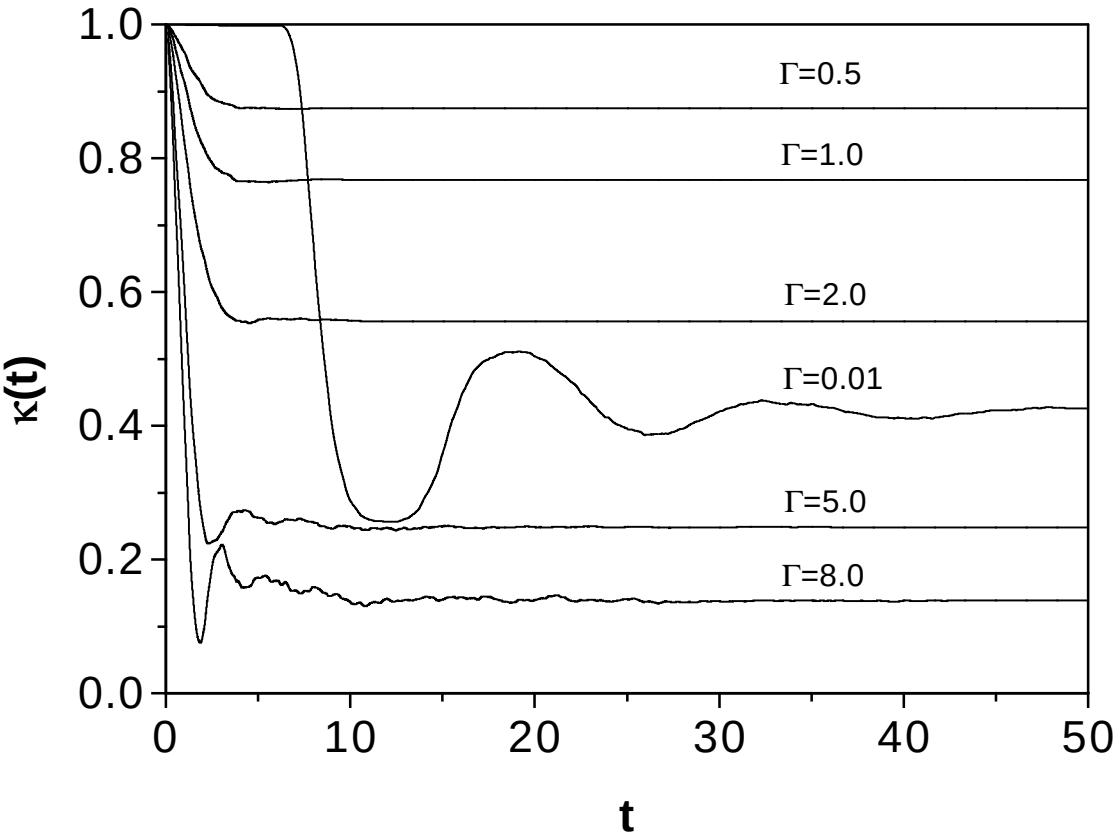

Fig.5

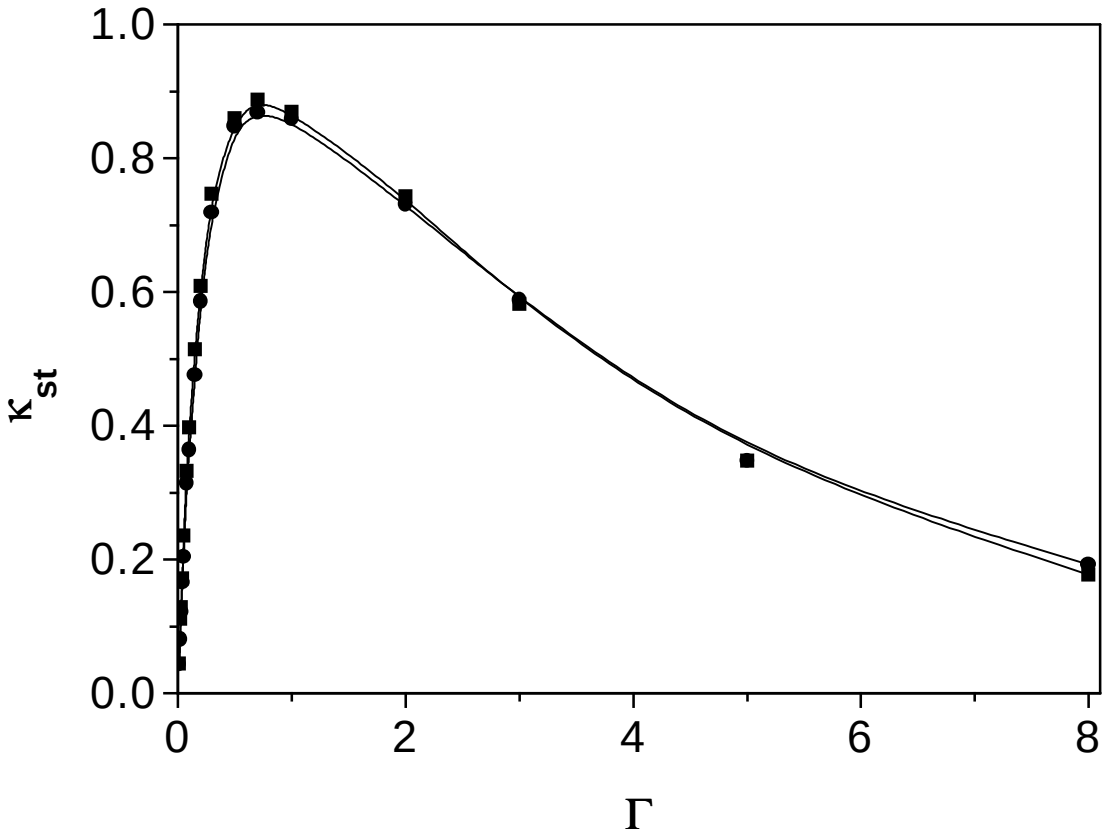

Fig.6

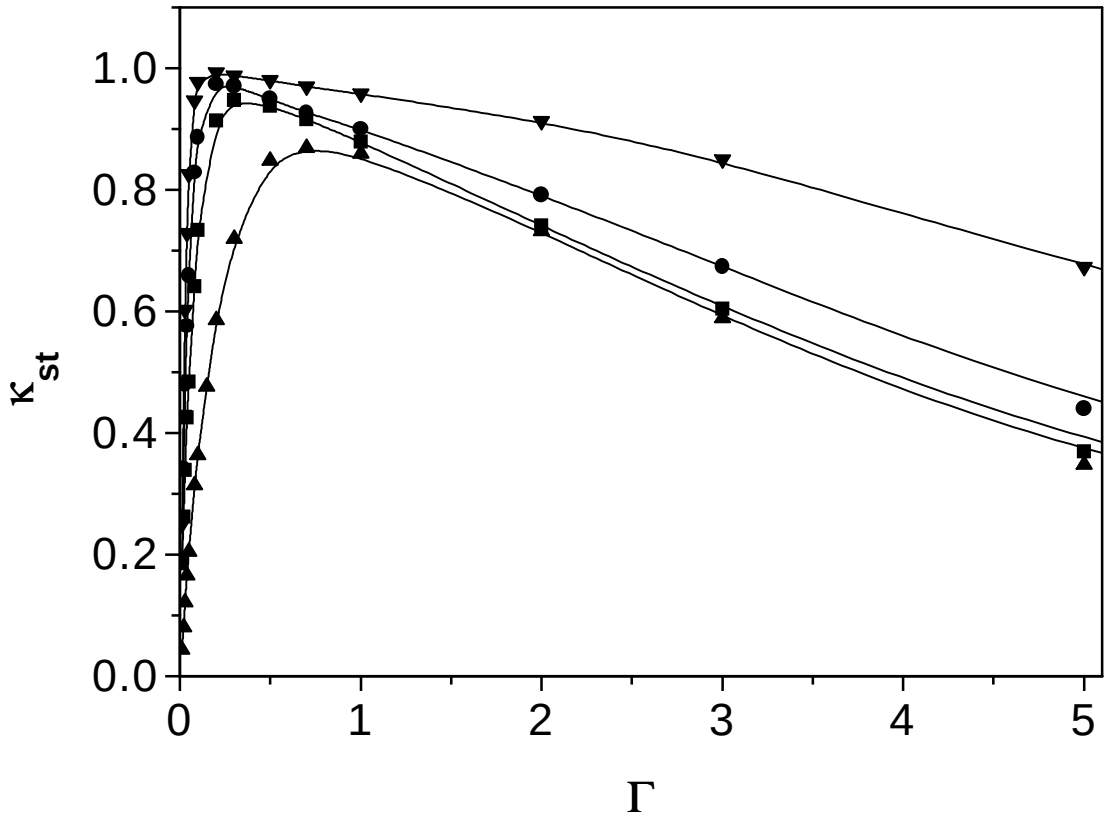

Fig.7

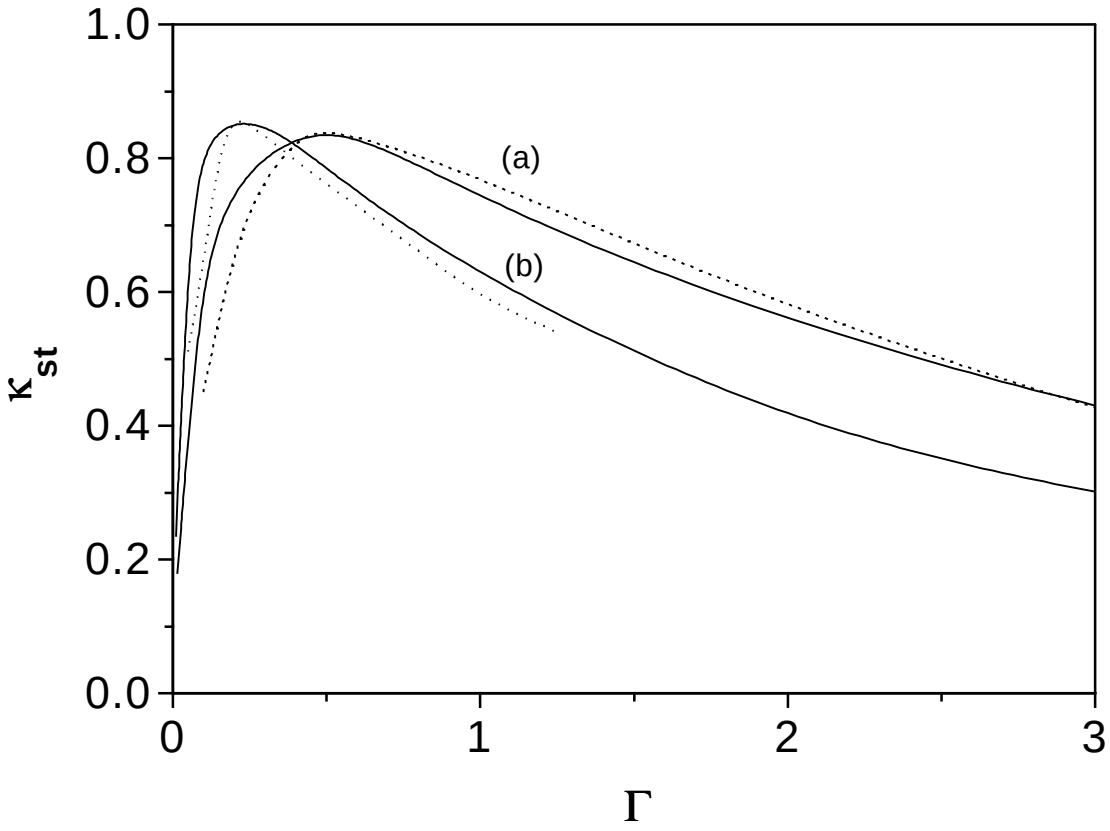

Fig.8

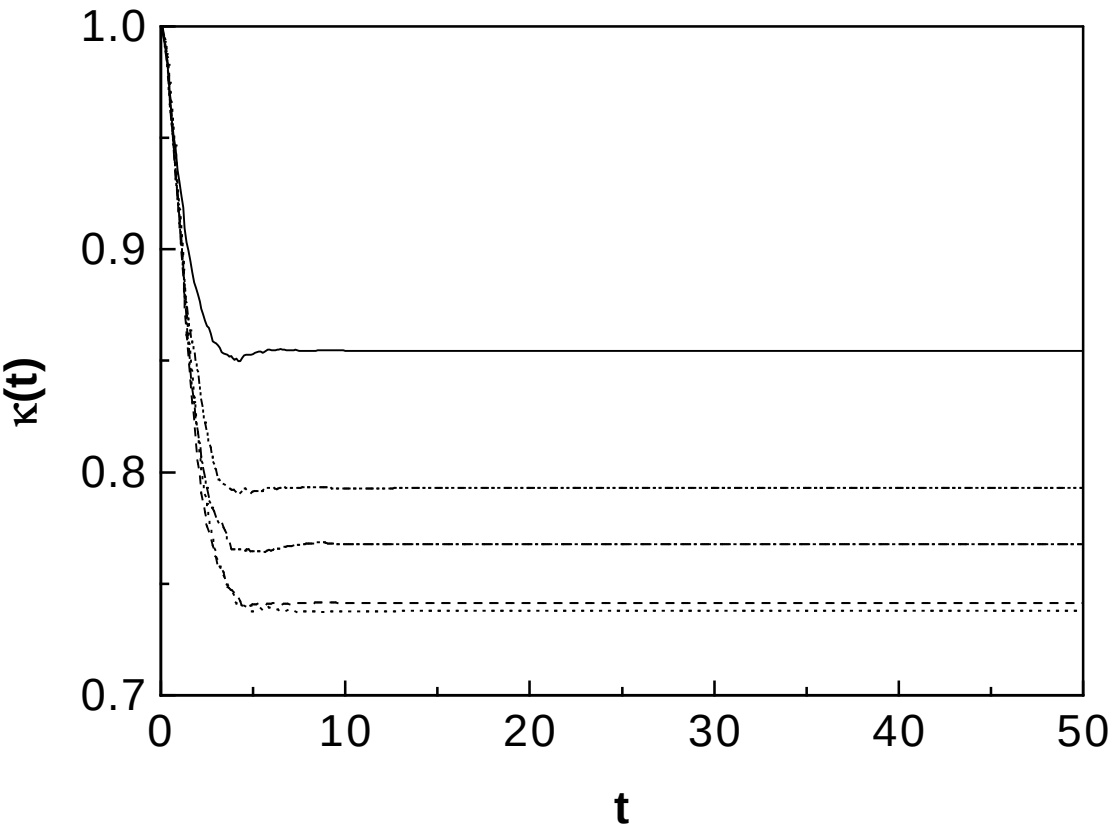

Fig.9

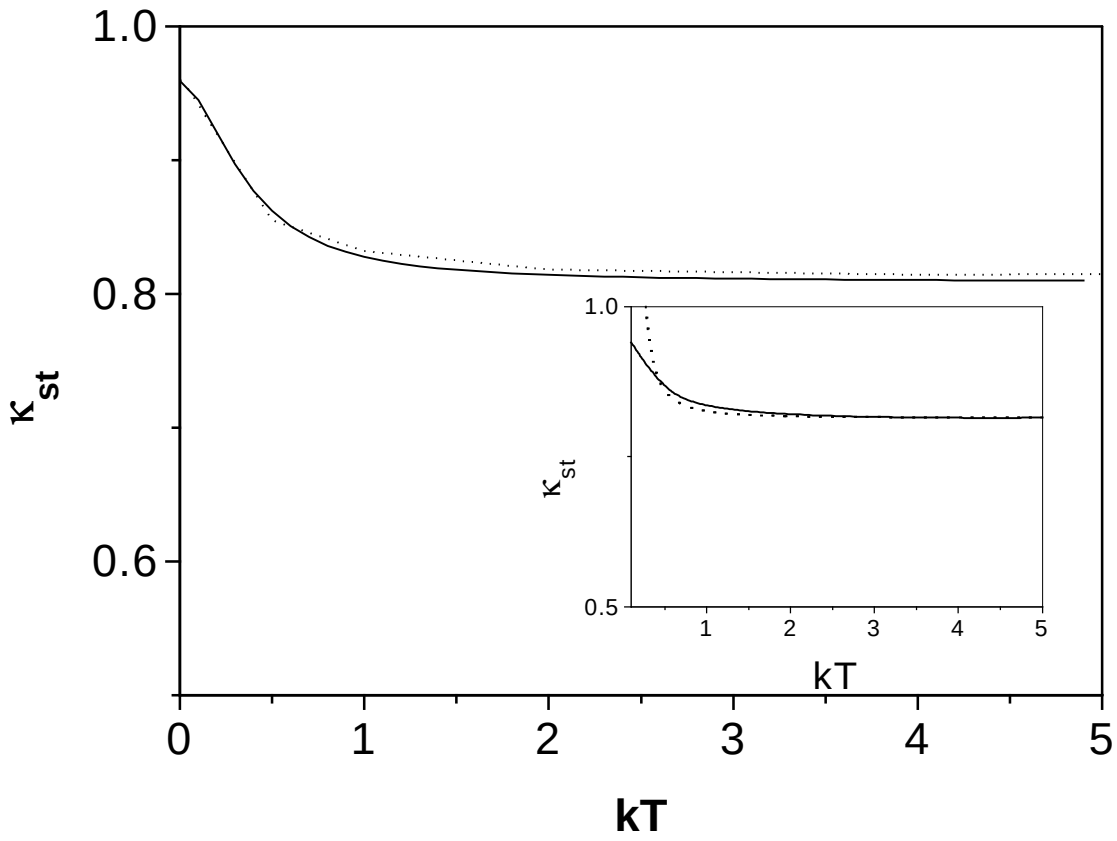

Fig.10

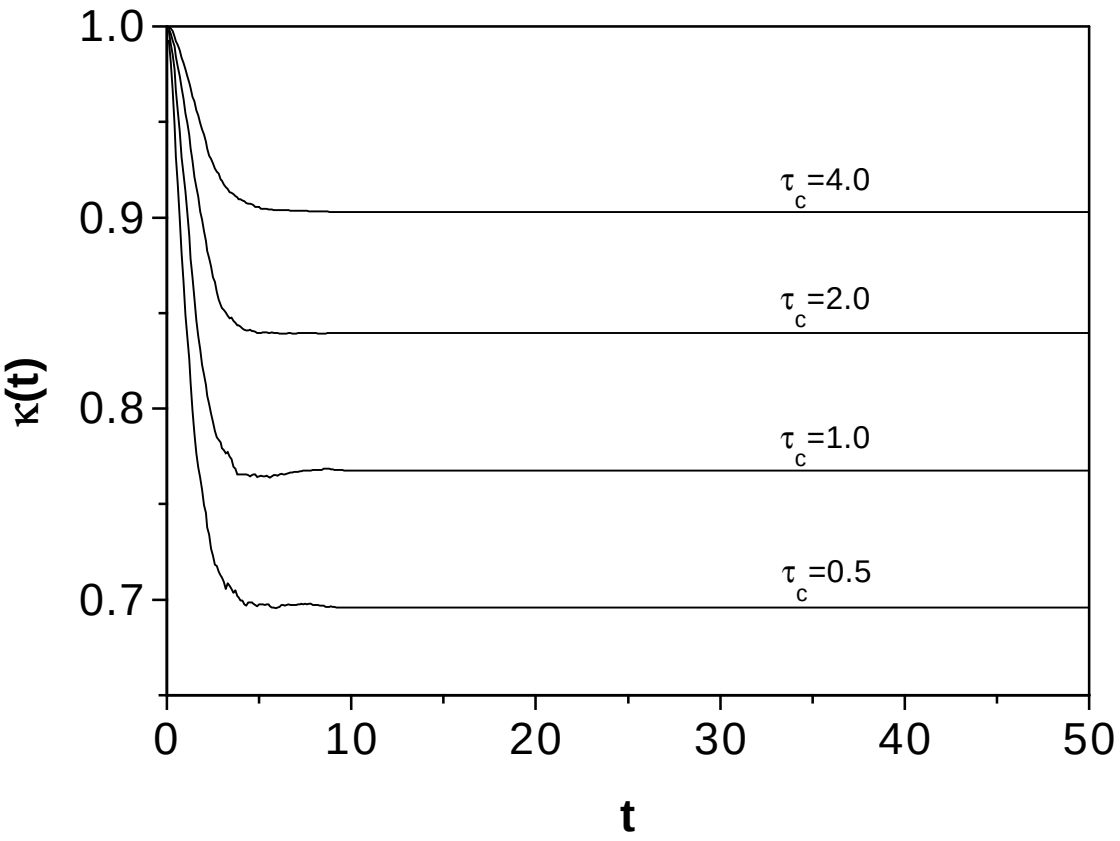

Fig.11